

Biaxial extension of a plane single crystal

K. MERABET¹⁾, A. CHENAOU¹⁾, F. SIDOROFF²⁾,
M. DARRIEULAT³⁾

¹⁾*E.M.P.M.H., Faculté des Sciences et Techniques de Tanger
B.P. 416, Tanger, Maroc, e-mail: a_chenaoui@yahoo.fr*

²⁾*LTDS, UMR, C.N.R.S. 5513, Ecole Centrale de Lyon
B.P. 163, 69131 Ecully Cedex, France*

³⁾*SMS, M.M.F., U.R.A., C.N.R.S. 1884,
Ecole Nationale Supérieure des Mines de Saint Etienne
158 cours Fauriel, 42023 Saint Etienne Cedex 2, France*

THIS PAPER CONCERNS the rigid-plastic modelisation of a f.c.c. single crystal, deforming by crystallographic slip, under large strain. Adopting the plane single crystal model, which corresponds to a true two-dimensional evolution of a real three-dimensional crystal, the activity of slip systems and the plastic indetermination, due to multiplicity of solutions, are studied according to the rate-independent Schmid law or the rate-dependent Bingham law. To promote a more general situation of potential multiple slip and therefore of potential indeterminacy, the biaxial loading is investigated. Based on this model and the Bingham slip law, the indeterminacy problem is surmounted, by adopting the geometrical analysis in the strain rate space and it is proved that the linear viscoplastic analysis is a new way of solving the indeterminacy problem.

Key words: crystal plasticity, metallic materials, viscoplastic material, finite strain.

Notations

\mathbf{F}	deformation gradient tensor,
\mathbf{P}	plastic transformation tensor,
\mathbf{R}	lattice rotation tensor,
\mathbf{L}	velocity gradient tensor,
\mathbf{D}	strain rate tensor,
\mathbf{W}	rotation rate tensor,
$\overline{\mathbf{D}}$	strain rate tensor rotated in the crystallographic configuration,
$\overline{\mathbf{W}}$	rotation rate tensor rotated in the crystallographic configuration,
\mathbf{T}	Cauchy stress tensor,
$\overline{\mathbf{T}}$	Cauchy stress tensor rotated in the crystallographic configuration,
$\overline{\mathbf{N}}^s$	the s -th “pseudo slip” system,
$\dot{\alpha}^s$	shear strain rate on the “pseudo slip” system (s),
σ^s	resolved shear stress on the “pseudo slip” system (s),
τ_c	critical resolved shear stress,
$\bar{x}_1, \bar{x}_2, \bar{x}_3$	space coordinates in the crystallographic frame,
θ	orientation of the laboratory frame.

1. Introduction

MOST MATERIALS, NOWADAYS used, are polycrystalline aggregates defined by microstructure and crystallographic texture. Under such circumstances, it is useful to describe the macroscopic behavior of a particular piece of material, as an average of the microscopic behavior, which has been taken over the constituent grains. The single crystal therefore should play an important role in describing the deformation behavior of metallic materials and in understanding the microstructure and texture effect on mechanical properties during the industrial processes.

The single crystal behavior has been widely studied. The quantitative description of plastic flow by crystallographic slip may be traced back to early works of [1–4]. Constitutive equations for elasto-plastic behaviour of ductile single crystals from the standpoint of modern continuum mechanics were first formulated by [5] and [6], and extended to finite deformation by [7–13].

In these formulations, if the mechanics of single crystal is clearly formulated, many problems have not been completely solved. For instance, in the classical rate-independent theory, the limitation stems essentially from a loss of uniqueness of the mode of slip, corresponding to the choice of active slip systems [14] and [15]. This is a well-known difficulty in rate-independent crystalline plasticity that has also been of particular concern, for example, in texture analyses. The prediction of texture in single crystals or polycrystals requires a precise specification of the slip mode to calculate lattice and grain rotation. To overcome this well-known indetermination problem, the comparison between rate-sensitive and rate-insensitive behaviour is also an important issue.

For single crystal plasticity models, the studies in three dimensions seldom lead to analytical solutions. However, this is desirable because it puts into evidence the role played by the various factors influencing the deformation: sets of active slip systems, lattice rotation and strain hardening.

To bypass this complexity, typically, an analysis in two dimensions has been widely overviewed in different papers and used for gaining a greater physical insight. [11] and [16] used idealized symmetry double-slip models, obtained an analytical solution for bifurcation of a shear band in ductile single crystal under uniaxial tension and proved that shear banding is possible with positive hardening.

In another work, based on the double-slip kinematics, DAFALIAS [17] integrated analytically the CLEMENTS equation [18] and obtained the ODF expression. This was used to describe the related texture development. Also, it has been shown that it could be possible to obtain exact analytical expression describing the stress-strain response and the yield-surface evolution of a polycrystal under general large plane deformation.

Another plane single crystal model was proposed by [19] and [20], corresponding to a single crystal when solicited in a material symmetry plane (in cubic metals, a $\{100\}$ or $\{110\}$ one). This model, which is presented in the formalism of large deformations, is based on the fact that the material plane remains an element of symmetry throughout the loading strain path. The full advantage of such two-dimensional model is its ability and simplicity to describe some forming process and can be directly used, for example, to study the mechanical behaviour of grains in a rolled sheet with a Cube, Goss or Copper orientations. In the framework of this model, simple shear, biaxial stretching [21] and the uniaxial tension [22], have already been investigated, for assessing the plastic spin and the texture analysis and the dependence of the threshold of strain localization on a combination of crystal rotation and strain hardening effects.

The present paper deals with biaxial extension. Our main objective is a theoretical study of slip systems activity and crystal orientation evolution, in the rate-independent or rate-dependent behaviour. This is essential to analyse the intriguing influence of the anisotropic development and the straining path on the plastic spin.

Firstly, as a comparison basis, part of the calculations is presented with the Schmid law and uniform strain hardening in the biaxial extension test. Based on the plane projective representation in strain space [21], the geometrical analysis is used for determining the sets of active slip systems in terms of the lattice orientation and the strain path loading.

Secondly, the choice for the rate-sensitive behaviour has been followed for solving the ambiguities within the frame of rate-independent plasticity. In fact, many numerical solutions have been developed [23–24] with a power law relationship between the resolved shear stress and the rate slip. However, if such laws may be quite successful in many cases, they are not satisfactory because they do not take into account the core of the Schmid law, namely the existence of a critical resolved shear stress below which a slip system cannot be activated. The linear BINGHAM law [25], on the contrary, is representative of a rate-dependent Schmid law, and permits a complete resolution of the equations. In this paper, the Bingham law is used for solving the encountered indetermination problem, caused by the rate-independent plasticity.

2. Mechanical framework

2.1. Plane single crystal

A single crystal is a three-dimensional anisotropic material. In general, a two-dimensional strain states will result in a three-dimensional stress and vice-versa. This difficulty is usually skipped by considering some fictitious two-dimensional crystal (double slip model ([11, 26] and [27])).

However, if the 3D single crystal is considered in one of its symmetry planes, then plane stress and plane strain are compatible resulting in a true two-dimensional model: “The plane single crystal” which is defined by the kinematical equations

$$\mathbf{F} = \mathbf{R}\mathbf{P},$$

$$\dot{\mathbf{P}}\mathbf{P}^{-1} = \sum_s^m \dot{\alpha}^s \bar{\mathbf{N}}^s,$$

where \mathbf{F} , \mathbf{P} and \mathbf{R} respectively denote the deformation gradient, the plastic transformation and the lattice rotation tensors, while $\bar{\mathbf{N}}^s$ is the plane pseudo-slip system, defined in the crystallographic (isoclinic) configuration, which represents the symmetric contribution of two systems symmetric to $\dot{\mathbf{P}}\mathbf{P}^{-1}$ ([19–21], [28–29]).

The velocity gradient \mathbf{L} , strain rate $\mathbf{D} = (\mathbf{L})^S$ and rotation rate $\mathbf{W} = (\mathbf{L})^A$ then result as

$$L = \dot{\mathbf{F}}\mathbf{F}^{-1} = \dot{\mathbf{R}}\mathbf{R}^T + \mathbf{R}\dot{\mathbf{P}}\mathbf{P}^{-1}\mathbf{R}^T,$$

$$(2.1) \quad \bar{\mathbf{D}} = \mathbf{R}^T \mathbf{D} \mathbf{R} = \sum_s^m \dot{\alpha}^s (\bar{\mathbf{N}}^s)^S,$$

$$(2.2) \quad \bar{\mathbf{W}} = \mathbf{R}^T \mathbf{W} \mathbf{R} = \mathbf{R}^T \dot{\mathbf{R}} + \sum_s^m \dot{\alpha}^s (\bar{\mathbf{N}}^s)^A,$$

where suffix $()^S$ and $()^A$ respectively denote the symmetric and skew-symmetric part of any tensor and where a superimposed bar denotes tensors rotated in the crystallographic configuration.

The applied resolved shear stress on any (s) pseudo-slip system can be written as

$$\sigma^s = \bar{\mathbf{T}} \bar{\mathbf{N}}^s, \quad \bar{\mathbf{T}} = \mathbf{R}^T \mathbf{T} \mathbf{R},$$

where \mathbf{T} is the usual Cauchy stress tensor observed in the laboratory frame and $\bar{\mathbf{T}}$ is the corresponding tensor in the crystallographic frame.

In this plane case, the lattice rotation \mathbf{R} and the Cauchy stress tensor \mathbf{T} are given by

$$\mathbf{R} = \begin{bmatrix} \cos(\theta) & \sin(\theta) & 0 \\ -\sin(\theta) & \cos(\theta) & 0 \\ 0 & 0 & 1 \end{bmatrix}, \quad \mathbf{R}^T \dot{\mathbf{R}} = \dot{\theta} \begin{bmatrix} 0 & 1 & 0 \\ -1 & 0 & 0 \\ 0 & 0 & 0 \end{bmatrix}, \quad \mathbf{T} = \begin{bmatrix} \sigma_1 & \tau & 0 \\ \tau & \sigma_2 & 0 \\ 0 & 0 & 0 \end{bmatrix};$$

θ defines the plane rotation between laboratory frame and crystallographic frame. The isoclinic stress tensor $\bar{\mathbf{T}}$ is defined as

$$\bar{T}_{11} = \frac{\sigma_1 + \sigma_2}{2} + \frac{\sigma_1 - \sigma_2}{2} \cos(2\theta) - \tau \sin(2\theta),$$

$$\bar{T}_{22} = \frac{\sigma_1 + \sigma_2}{2} - \frac{\sigma_1 - \sigma_2}{2} \cos(2\theta) + \tau \sin(2\theta),$$

$$\bar{T}_{12} = \frac{\sigma_1 - \sigma_2}{2} \sin(2\theta) + \tau \cos(2\theta).$$

These kinematic equations (2.1) and (2.2), are completed by N slip laws relating, on each slip system, the slip rate $\dot{\alpha}^s$ to the resolved shear stress σ^s . Two cases will be considered in the following:

- Schmid's slip law

$$(2.3) \quad \begin{aligned} \dot{\alpha}^s &\geq 0 & \text{if} & \quad \sigma^s = \tau_c, \\ \dot{\alpha}^s &= 0 & \text{if} & \quad |\sigma^s| \leq \tau_c, \\ \dot{\alpha}^s &\leq 0 & \text{if} & \quad \sigma^s = -\tau_c. \end{aligned}$$

- Viscoplastic law of Bingham type

$$(2.4) \quad \sigma^s = (\tau_c + \mu|\dot{\alpha}^s|) \operatorname{sgn}(\dot{\alpha}^s)$$

with the same critical shear stress τ_c for all systems.

Together, the kinematical relations (2.1), (2.2) and slip law ((2.3) or (2.4)), provide $N + 4$ equations which, for a prescribed deformation history \mathbf{F} , will give $N + 4$ unknowns which are N slip rates $\dot{\alpha}^s$, 3 components of stress ($\bar{T}_{11}, \bar{T}_{22}, \bar{T}_{12}$) and the lattice rotation $\dot{\theta}$.

2.2. The f.c.c.P2 plane single crystal

The f.c.c.P2 model is the plane single crystal corresponding to a plane stress and strain state in the $\{110\}$ planes. In this case the crystallographic frame $(\bar{x}_1, \bar{x}_2, \bar{x}_3)$ is chosen

$$\bar{x}_1 = [001], \quad \bar{x}_2 = [1\bar{1}0], \quad \bar{x}_3 = [110].$$

The corresponding pseudo-slip systems are summarized in Table 1. This table is obtained by noting that, under plane stress and strain, two true systems disappear (because the corresponding resolved shear stress vanishes) and ten remaining true systems can be symmetrized into five plane pseudo-slip systems. For further details, the reader is referred to [19] and [21].

Finally, for this model the kinematical relations (2.1) and (2.2) become

$$(2.5) \quad \begin{aligned} \bar{D}_{11} &= \frac{1}{\sqrt{6}}(\dot{\alpha}^3 + \dot{\alpha}^4 - \dot{\alpha}^5 - \dot{\alpha}^2), \\ \bar{D}_{22} &= \frac{1}{\sqrt{6}}(\dot{\alpha}^5 - \dot{\alpha}^4), \\ \bar{D}_{12} &= \frac{1}{4\sqrt{3}}(2\dot{\alpha}^1 + \dot{\alpha}^2 + \dot{\alpha}^3 + \dot{\alpha}^4 + \dot{\alpha}^5), \end{aligned}$$

Table 1. f.c.c.P2 single crystal.

True systems (Bishop and Hill notation)	Pseudo system (s)	Pseudo-slip $\bar{\mathbf{N}}^s$	Resolved shear σ^s
$(a_3, -b_3)$	1	$\bar{\mathbf{N}}^1 = \frac{1}{2\sqrt{3}} \begin{bmatrix} 0 & 0 \\ 2 & 0 \end{bmatrix}$	$\sigma^1 = \frac{\bar{T}_{12}}{\sqrt{3}}$
$(-a_2, -b_1)$	2	$\bar{\mathbf{N}}^2 = \frac{1}{2\sqrt{3}} \begin{bmatrix} -\sqrt{2} & 0 \\ 1 & 0 \end{bmatrix}$	$\sigma^2 = \frac{\bar{T}_{12} - \sqrt{2}\bar{T}_{11}}{2\sqrt{3}}$
$(-a_1, -b_2)$	3	$\bar{\mathbf{N}}^3 = \frac{1}{2\sqrt{3}} \begin{bmatrix} \sqrt{2} & 0 \\ 1 & 0 \end{bmatrix}$	$\sigma^3 = \frac{\bar{T}_{12} + \sqrt{2}\bar{T}_{11}}{2\sqrt{3}}$
$(d_2, -d_1)$	4	$\bar{\mathbf{N}}^4 = \frac{1}{2\sqrt{3}} \begin{bmatrix} \sqrt{2} & 2 \\ -1 & -\sqrt{2} \end{bmatrix}$	$\sigma^4 = \frac{\bar{T}_{12} + \sqrt{2}(\bar{T}_{11} - \bar{T}_{22})}{2\sqrt{3}}$
$(c_1, -c_2)$	5	$\bar{\mathbf{N}}^5 = \frac{1}{2\sqrt{3}} \begin{bmatrix} -\sqrt{2} & 2 \\ -1 & \sqrt{2} \end{bmatrix}$	$\sigma^5 = \frac{\bar{T}_{12} - \sqrt{2}(\bar{T}_{11} - \bar{T}_{22})}{2\sqrt{3}}$

$$(2.6) \quad W_{12} = \dot{\theta} + \omega^p,$$

with

$$\omega^p = \frac{1}{4\sqrt{3}}(3\dot{\alpha}^4 + 3\dot{\alpha}^5 - 2\dot{\alpha}^1 - \dot{\alpha}^2 - \dot{\alpha}^3).$$

For the given kinematics, we then have to solve Eqs. (2.5) and (2.6) for eight unknowns; five slip rates $\dot{\alpha}^s$ and three components $(\bar{T}_{11}, \bar{T}_{22}, \bar{T}_{12})$, while the lattice spin $\dot{\theta}$ is obtained afterwards from the relation (2.6). Of course, it is not possible to obtain the five $\dot{\alpha}^s$ from the three Eqs. (2.5). However, it will be convenient to solve these three equations in the following form:

$$(2.7) \quad \begin{aligned} \dot{\alpha}^1 &= \frac{\sqrt{3}}{2} (3\bar{D}_{12} - \omega^p - \xi), \\ \dot{\alpha}^2 &= \frac{\sqrt{3}}{2} [\xi - \sqrt{2}(\bar{D}_{11} + \bar{D}_{22})], \\ \dot{\alpha}^3 &= \frac{\sqrt{3}}{2} [\xi + \sqrt{2}(\bar{D}_{11} + \bar{D}_{22})], \\ \dot{\alpha}^4 &= \frac{\sqrt{3}}{2} (\bar{D}_{12} + \omega^p - \sqrt{2}\bar{D}_{22}), \\ \dot{\alpha}^5 &= \frac{\sqrt{3}}{2} (\bar{D}_{12} + \omega^p + \sqrt{2}\bar{D}_{22}), \end{aligned}$$

which gives $\dot{\alpha}^s$ in terms of $\bar{\mathbf{D}}$ and two indeterminate quantities ξ and ω^p .

2.3. Strain rate representation

The CFPCP2 rigid plastic model case has been analysed in [19] for a rate-independent behaviour. An appropriate geometric representation of the strain rate is obtained by starting from the three-dimensional space (Y_1, Y_2, Y_3) defined as

$$(2.8) \quad Y_1 = \bar{D}_{11}, \quad Y_2 = \bar{D}_{22}, \quad Y_3 = \sqrt{2}\bar{D}_{12}$$

and remarking that, for a rate-independent material, it is only the direction of the corresponding vector which is meaningful. It is then convenient to represent this space by two parallel planes, for instance the planes $Y_3 = \pm 1$. In this representation, one direction in the strain rate space is represented by one point, with the exception of the directions in the (Y_1, Y_2) plane, corresponding to $Y_3 = 0$, which are rejected to infinity (projective geometry). This diagram is constructed from the yield polyhedron [19] corresponding to the condition $\sigma^s = \pm\tau_c$ for the five pseudo-slip systems defined in Table 1. Each node in this diagram corresponds to the activity of one system. For instance, the node 1^+ ($Y_1 = Y_2 = 0$ in the $Y_3 = +1$ plane) corresponds to $\sigma^1 = +\tau_0$, the node 5^- (in the $Y_3 = -1$ plane) corresponds to $\sigma^5 = -\tau_0$... etc. Similarly, each segment corresponds to the activity of two systems (1^+ and 5^+ on the segment 1^+5^+) and each surface — to the activity of three or more systems. This diagram is presented in Fig. 1 and the reader is referred to [19] and [21] for a precise construction.

For each value of $\bar{\mathbf{D}}$ the representative point, in these planes, describes the curve when Y_1 and Y_2 change, which gives the active systems.

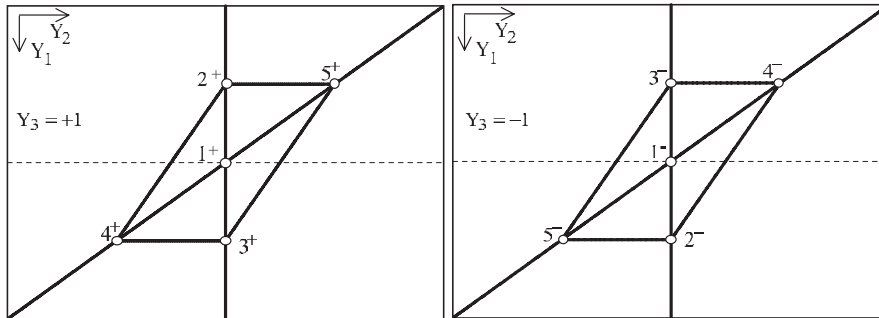


FIG. 1.

3. The biaxial extension

Now we shall focus our attention on the biaxial extension which is defined as

$$\mathbf{F} = \begin{bmatrix} e^\varepsilon & 0 & 0 \\ 0 & e^{\rho\varepsilon} & 0 \\ 0 & 0 & e^{-(1+\rho)\varepsilon} \end{bmatrix}, \quad \mathbf{L} = \begin{bmatrix} 1 & 0 & 0 \\ 0 & \rho & 0 \\ 0 & 0 & -(1+\rho) \end{bmatrix} E,$$

where $E = \dot{\epsilon}$ is the stretching rate and ρ is the strain ratio defined in the range $-1 \leq \rho \leq 1$.

The component W_{12} of $\overline{\mathbf{W}}$ is constantly zero ($W_{12} = 0$) and the strain rate $\overline{\mathbf{D}}$ in the three-dimensional space (Y_1, Y_2, Y_3) is

$$(3.1) \quad \begin{aligned} Y_1 &= \left(\frac{1+\rho}{2} + \frac{1-\rho}{2} \cos(2\theta) \right) E, \\ Y_2 &= \left(\frac{1+\rho}{2} - \frac{1-\rho}{2} \cos(2\theta) \right) E, \\ Y_3 &= \left(\sqrt{2} \frac{1-\rho}{2} \sin(2\theta) \right) E, \end{aligned}$$

and it depends on the lattice rotation θ which is unknown.

3.1. The plastic analysis

According to (3.1), biaxial extension is given in the projective geometric representation $Y_3 = \pm 1$, described above, by the following equations:

$$(3.2) \quad \begin{aligned} Y_1 &= \pm \frac{\sqrt{2}}{2} \left\{ A(\rho) \frac{1}{\sin(2\theta)} + \frac{1}{\tan(2\theta)} \right\}, \\ Y_2 &= \pm \frac{\sqrt{2}}{2} \left\{ A(\rho) \frac{1}{\sin(2\theta)} - \frac{1}{\tan(2\theta)} \right\}, \end{aligned}$$

symbol $+$ if $Y_3 = +1$ with $\sin(2\theta) \geq 0$ and symbol $-$ if $Y_3 = -1$ with $\sin(2\theta) \leq 0$. Here $A(\rho) = (1 + \rho)/(1 - \rho)$ with $0 \leq A(\rho) \leq \infty$.

For each value of ρ , the relations (3.2) define, in terms of θ , the strain rate curve in the plane (Y_1, Y_2) . The biaxial analysis follows from the superposition of this curve, representing the prescribed kinematics, with the constitutive diagram of Fig. 1, which characterizes the considered plane single crystal. The results are presented in Fig. 2. For $\rho = -1$, this case corresponds to the stretching biaxial test, which is mostly studied in [21]. For $\rho \neq -1$, according to the values of ρ and θ , two situations may be encountered:

- an apex which corresponds to 3 pseudo-slip active systems; in this case there is no slip indetermination and the rotation is completely determined;
- an apex which corresponds to 4 pseudo-slip active systems leading to the slip indetermination (3 equations from $\overline{\mathbf{D}}$ (2.5) for 4 unknown slip rate $\dot{\alpha}^s$).

In this analysis we shall concentrate on the particular case of the apex with 4 slip systems. Precisely, as shown in [19], for a CFCP2 rigid-plastic model used here, this variety of apexes corresponds to activation of systems 2, 3, 4 and 5 and

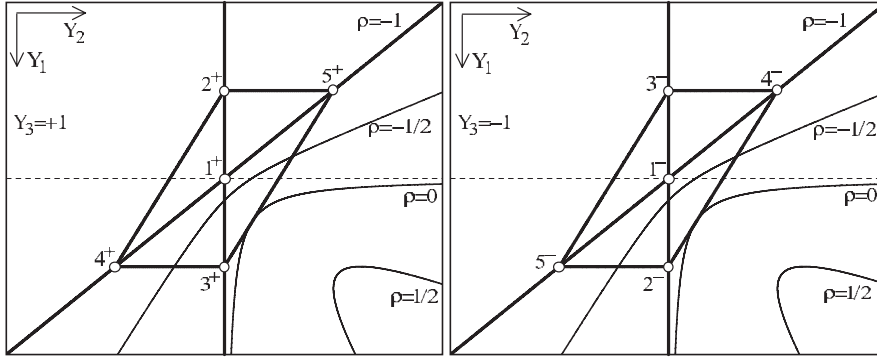


FIG. 2.

nonactivation of system 1 with $\dot{\alpha}^1 = 0$. The kinematic relation (2.7) then allows the determination of the four unknown slip rates $\dot{\alpha}^2, \dot{\alpha}^3, \dot{\alpha}^4, \dot{\alpha}^5$ as functions of one quantity which for instance can be taken as the spin ω^p occurring in

$$\begin{aligned}
 \dot{\alpha}^2 &= \frac{\sqrt{3}}{2} \left[-\omega^p + 3\bar{D}_{12} - \sqrt{2}(\bar{D}_{11} + \bar{D}_{22}) \right], \\
 \dot{\alpha}^3 &= \frac{\sqrt{3}}{2} \left[-\omega^p + 3\bar{D}_{12} + \sqrt{2}(\bar{D}_{11} + \bar{D}_{22}) \right], \\
 \dot{\alpha}^4 &= \frac{\sqrt{3}}{2} \left(\omega^p + \bar{D}_{12} - \sqrt{2}\bar{D}_{22} \right), \\
 \dot{\alpha}^5 &= \frac{\sqrt{3}}{2} \left(\omega^p + \bar{D}_{12} + \sqrt{2}\bar{D}_{22} \right).
 \end{aligned}
 \tag{3.3}$$

The plastic spin, and therefore the lattice spin $\dot{\theta}$ by (2.6), remain indeterminate, except for the activity condition of each apex. For instance, for $2^-3^+4^+5^-$ combination, this activity condition is written as

$$\dot{\alpha}^2 \leq 0, \quad \dot{\alpha}^3 \geq 0, \quad \dot{\alpha}^4 \geq 0, \quad \dot{\alpha}^5 \leq 0,$$

which reduces to the following inequalities representing the infinity solution for ω^p

$$\begin{aligned}
 |\omega^p - 3\bar{D}_{12}| &\leq \sqrt{2}(\bar{D}_{11} + \bar{D}_{22}), \\
 |\omega^p + \bar{D}_{12}| &\leq -\sqrt{2}\bar{D}_{22}.
 \end{aligned}
 \tag{3.4}$$

Using (3.1), the relation (3.4)₂ impose that $\bar{D}_{22} \leq 0$. According to the sign of \bar{D}_{12} , three solutions are possible and the set of different slip rates combinations is given as:

- For $\bar{D}_{12} \geq 0$ or $\sin(2\theta) \geq 0$, only the following set is possible:

$$S_1 = \{(2^-3^+4^+5^-), (3^+4^+5^-), (2^-3^+5^-)\}.$$

- For $\bar{D}_{12} \leq 0$ or $\sin(2\theta) \leq 0$, only the following set is possible:

$$S_2 = \{(2^-3^+4^+5^-), (2^-4^+5^-), (2^-3^+4^+)\}.$$

It should be noted that for S_1 and S_2 the difficulty subsists in the choice of the corresponding combination. Consequently, to select the active slip systems we use in this work the usual criterion of the Taylor principle of minimum of the internal plastic work dissipation $\dot{\omega}$ which, in the isotropic hardening case, is defined as

$$\dot{\omega} = \sum \tau_c |\dot{\alpha}^s|,$$

which gives, by using (3.3), for each combination of S_1 or S_2

$$\dot{\omega} = \sqrt{6}\tau_c \bar{D}_{11}.$$

We obtain the same plastic work dissipation for all possible solutions. This shows that the proposed criterion, generally, is not adequate for solving the indeterminacy problem encountered in the case of rate-independent behaviour.

3.2. The viscoplastic analysis

The viscoplastic Bingham law (2.4) takes on the three different linear analytical forms according to the value of σ^s and $\dot{\alpha}^s$:

$$(3.5) \quad \begin{array}{ll} + & \sigma^s = \tau_c + \mu \dot{\alpha}^s \quad \dot{\alpha}^s \geq 0, \\ 0 & |\sigma^s| \leq \tau_c \quad \dot{\alpha}^s = 0, \\ - & \sigma^s = -\tau_c + \mu \dot{\alpha}^s \quad \dot{\alpha}^s \leq 0, \end{array}$$

each of them being characterized by one equality and one inequality.

The activity regime is therefore defined by the activity from +, 0 or -, assumed for each of the five slip systems. Each activity regime can easily be analysed by solving the linear system obtained from (3.5) and the appropriate equality (2.7). The corresponding inequality can then be used for assessing the validity range of this particular regime.

The essential problem therefore is the determination of the activity regime associated with each deformation rate. More generally, the behaviour of the viscoplastic single crystal remains true in the plastic case for small rates and the relative part of viscous contribution increases with the strain rate. In this case the viscoplastic solution is the same as in the plastic case, corresponding to a succession of plastic regimes.

In the following, we shall focus our attention on the plastic regimes in the Bingham law framework for analysing the encountered indetermination problem. Let us now come back to the slip indetermination problem obtained in the above plastic case. The plastic analysis showed the potential activation of four systems $2^-3^+4^+5^-$ with the associated indetermination. Therefore, we shall introduce the viscoplastic analysis by the $0-++-$ regime; with obvious notations: system 1 not activated, systems 2 and 5 in $-$ mode and systems 3 and 4 in $+$ mode.

Combining (3.5) and (3.3), the corresponding linear system is written as

$$\begin{aligned}
 \dot{\alpha}^1 &= \frac{\sqrt{3}}{2}(3\bar{D}_{12} - \omega^p - \xi) = 0, \\
 \dot{\alpha}^2 &= \frac{\sqrt{3}}{2}(\xi - \sqrt{2}(\bar{D}_{11} + \bar{D}_{22})) = \frac{1}{\mu}(\sigma^2 + \tau_c), \\
 \dot{\alpha}^3 &= \frac{\sqrt{3}}{2}(\xi + \sqrt{2}(\bar{D}_{11} + \bar{D}_{22})) = \frac{1}{\mu}(\sigma^3 - \tau_c), \\
 \dot{\alpha}^4 &= \frac{\sqrt{3}}{2}(\bar{D}_{12} + \omega^p - \sqrt{2}\bar{D}_{22}) = \frac{1}{\mu}(\sigma^4 - \tau_c), \\
 \dot{\alpha}^5 &= \frac{\sqrt{3}}{2}(\bar{D}_{12} + \omega^p + \sqrt{2}\bar{D}_{22}) = \frac{1}{\mu}(\sigma^5 + \tau_c).
 \end{aligned}
 \tag{3.6}$$

The solution gives:

- The stress component \bar{T}_{12} :

$$\bar{T}_{12} = 6\mu\bar{D}_{12}.$$

- The plastic and lattice spin

$$\omega^p = \bar{D}_{12}, \quad \dot{\theta} = -\bar{D}_{12}.$$

- The pseudo-slip

$$\begin{aligned}
 \dot{\alpha}^2 &= \frac{\sqrt{3}}{2}(2\bar{D}_{12} - \sqrt{2}(\bar{D}_{11} + \bar{D}_{22})), \\
 \dot{\alpha}^3 &= \frac{\sqrt{3}}{2}(2\bar{D}_{12} + \sqrt{2}(\bar{D}_{11} + \bar{D}_{22})), \\
 \dot{\alpha}^4 &= \frac{\sqrt{3}}{2}(2\bar{D}_{12} - \sqrt{2}\bar{D}_{22}), \\
 \dot{\alpha}^5 &= \frac{\sqrt{3}}{2}(2\bar{D}_{12} + \sqrt{2}\bar{D}_{22}).
 \end{aligned}$$

These relations must be completed by the validity conditions

$$\dot{\alpha}^2 \leq 0, \quad \dot{\alpha}^3 \geq 0, \quad \dot{\alpha}^4 \geq 0, \quad \dot{\alpha}^5 \leq 0, \quad \sigma^1 = \left| \frac{\overline{T}_{12}}{\sqrt{3}} \right| \leq \tau_c.$$

Combining (2.8), the first four inequalities become in the (Y_1, Y_2, Y_3) space

$$Y_3 - Y_1 - Y_2 \leq 0,$$

$$Y_3 + Y_1 + Y_2 \geq 0,$$

$$Y_3 - Y_2 \geq 0,$$

$$Y_3 + Y_2 \leq 0,$$

and the last conditions require

$$|\sin(2\theta)| \leq \frac{\tau_c}{\sqrt{3}(1-\rho)\mu E},$$

what will be satisfied for $\mu E \rightarrow 0$.

So in the projective geometric representation $Y_3 = \pm 1$ we obtain

$$\pm 1 - Y_1 - Y_2 \leq 0,$$

$$\pm 1 + Y_1 + Y_2 \geq 0,$$

$$\pm 1 - Y_2 \geq 0,$$

$$\pm 1 + Y_2 \leq 0,$$

where the corresponding domain limit is represented in Fig. 3.

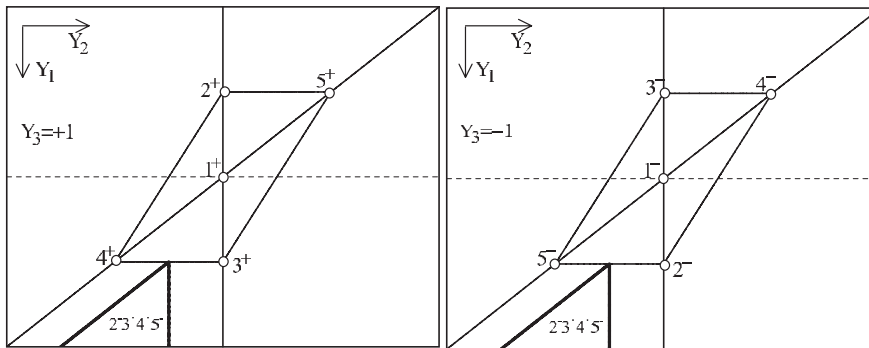


FIG. 3.

In the 0 - + + - regime this is the unique solution, but other regimes should be also investigated, in particular the regimes with three active systems which give rise to the limiting values in (3.4) and Fig. 3.

Let us consider for instance the viscoplastic regime 00 + + - corresponding to the non-activation of systems 1 and 2. The second equation in (3.6) has then to be replaced by $\dot{\alpha}^2 = 0$, so that the solution now is

$$\begin{aligned} \bar{T}_{12} &= 3\mu(4\bar{D}_{12} - \sqrt{2}(\bar{D}_{11} + \bar{D}_{22})), \\ \bar{T}_{11} &= 3\mu(-4\bar{D}_{12} + 3\sqrt{2}(\bar{D}_{11} + \bar{D}_{22})) + 2\sqrt{3}\tau_0, \\ \omega^p &= 3\bar{D}_{12} - \sqrt{2}(\bar{D}_{11} + \bar{D}_{22}), \\ \dot{\theta} &= -3\bar{D}_{12} + \sqrt{2}(\bar{D}_{11} + \bar{D}_{22}), \\ \dot{\alpha}^3 &= \frac{\sqrt{3}}{2}(2\sqrt{2}(\bar{D}_{11} + \bar{D}_{22})), \\ \dot{\alpha}^4 &= \frac{\sqrt{3}}{2}(4\bar{D}_{12} - 2\sqrt{2}\bar{D}_{22} - \sqrt{2}\bar{D}_{11}), \\ \dot{\alpha}^5 &= \frac{\sqrt{3}}{2}(4\bar{D}_{12} - \sqrt{2}\bar{D}_{11}), \end{aligned}$$

with the validity conditions

$$\dot{\alpha}^3 \geq 0, \quad \dot{\alpha}^4 \geq 0, \quad \dot{\alpha}^5 \leq 0,$$

$$\sigma^1 = \left| \frac{\bar{T}_{12}}{\sqrt{3}} \right| \leq \tau_c, \quad \sigma^2 = \left| \frac{\bar{T}_{12} - \sqrt{2}\bar{T}_{11}}{2\sqrt{3}} \right| \leq \tau_c,$$

which give the following inequalities:

$$\begin{aligned} 2\sqrt{2}(\bar{D}_{11} + \bar{D}_{22}) &\geq 0, \\ 4\bar{D}_{12} - 2\sqrt{2}\bar{D}_{22} - \sqrt{2}\bar{D}_{11} &\geq 0, \\ 4\bar{D}_{12} - \sqrt{2}\bar{D}_{11} &\leq 0, \\ \frac{\mu\sqrt{3}}{2}|4\bar{D}_{12} - 2\sqrt{2}\bar{D}_{22} - \sqrt{2}\bar{D}_{11}| &\leq \tau_0, \\ |\mu 2\sqrt{3}[2\bar{D}_{12} - \sqrt{2}(\bar{D}_{22} + \bar{D}_{11})] - \tau_0| &\leq \tau_0. \end{aligned}$$

The 5th condition is satisfied when $\mu E \rightarrow 0$, and the other inequalities reduce the (Y_1, Y_2, Y_3) -space to

$$\begin{aligned}
 (3.7) \quad & Y_1 + Y_2 \geq 0, \\
 & 2Y_3 - 2Y_2 - Y_1 \geq 0, \\
 & 2Y_3 - Y_1 \leq 0, \\
 & Y_3 - Y_1 - Y_2 \geq 0.
 \end{aligned}$$

The relations (3.7)₁ and (3.7)₄ mean that $Y_3 \geq 0$, so the corresponding domain limit is represented in the plane $Y_3 = +1$ (Fig. 4).

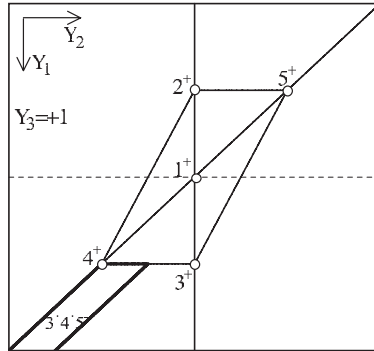


FIG. 4.

3.3. The adjusted plane projective

Other regimes can be analysed in the same way, leading to the entirely different limit domain constructed in Fig. 5, which corresponds to the new activity diagram in the strain-rate space. For each domain the associated rotation

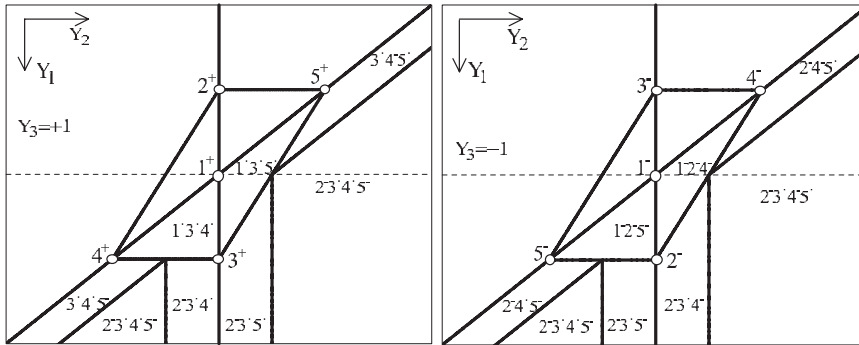


FIG. 5.

Table 2. Lattice rotation rate in terms of the system activity.

Zone	Rotation rate
$2^-3^+4^+5^-$	$\dot{\theta} = -\bar{D}_{12}$
$3^+4^-5^+$	$\dot{\theta} = -3\bar{D}_{12} + \sqrt{2}(\bar{D}_{11} + \bar{D}_{22})$
$2^-3^+4^+$	$\dot{\theta} = \bar{D}_{12} + \sqrt{2}\bar{D}_{22}$
$2^-4^+5^-$	$\dot{\theta} = -3\bar{D}_{12} - \sqrt{2}(\bar{D}_{11} + \bar{D}_{22})$
$2^-3^+4^-5^+$	$\dot{\theta} = -\bar{D}_{12}$
$3^+4^-5^-$	$\dot{\theta} = -3\bar{D}_{12} + \sqrt{2}(\bar{D}_{11} + \bar{D}_{22})$
$2^-3^+4^-$	$\dot{\theta} = \bar{D}_{12} + \sqrt{2}\bar{D}_{22}$
$2^-4^-5^+$	$\dot{\theta} = -3\bar{D}_{12} - \sqrt{2}(\bar{D}_{11} + \bar{D}_{22})$
$2^-3^+5^+$	$\dot{\theta} = \bar{D}_{12} - \sqrt{2}\bar{D}_{22}$
$1^+2^+4^+$	$\dot{\theta} = \bar{D}_{12} + \sqrt{2}\bar{D}_{22}$
$1^+3^+5^+$	$\dot{\theta} = \bar{D}_{12} - \sqrt{2}\bar{D}_{22}$
$1^-2^-4^-$	$\dot{\theta} = \bar{D}_{12} + \sqrt{2}\bar{D}_{22}$
$1^-2^-5^-$	$\dot{\theta} = \bar{D}_{12} - \sqrt{2}\bar{D}_{22}$

rate is summarized in Table 2. When the strain rate is imposed, this diagram gives the complete determination of the pseudo-slip systems.

4. Illustration

Using the adjusted activity diagram, for each value of ρ we determine a completely different activity system in terms of θ . As an illustrative example, we start from the axisymmetric deformation corresponding to $\rho = -1/2$. Using (3.1), this strain test is defined, in the strain rate space (Y_1, Y_2, Y_3) , by

$$Y_1 = \frac{1}{4}(1 + 3 \cos(2\theta))E,$$

$$Y_2 = \frac{1}{4}(1 - 3 \cos(2\theta))E,$$

$$Y_3 = +\frac{3\sqrt{2}}{4}(\sin(2\theta))E.$$

The corresponding curves in the adjusted plane projective representation are given in Fig. 6. When θ varies from 0 to π , the resulting systems activity are summarized in Table 3 with:

$$\tan(2\theta_1) = \frac{-\sqrt{2}A + \sqrt{3 - A^2}}{A + \sqrt{2}\sqrt{3 - A^2}}, \quad \tan(2\theta_2) = \frac{2\sqrt{2}A + \sqrt{9 - A^2}}{-A + 2\sqrt{2}\sqrt{9 - A^2}},$$

$$\tan(2\theta_3) = \frac{\sqrt{1 - A^2}}{A}, \quad \tan(2\theta_4) = \frac{2\sqrt{2}A + \sqrt{1 - A^2}}{A - 2\sqrt{2}\sqrt{1 - A^2}}, \quad \tan(2\theta_5) = \frac{\sqrt{2}A}{\sqrt{1 - 2A^2}}.$$

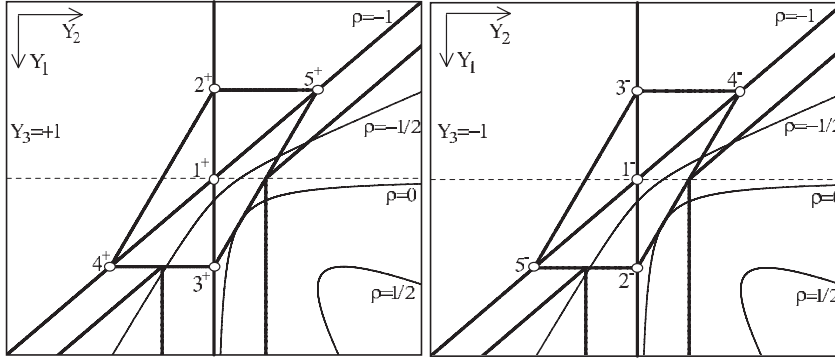


FIG. 6.

Table 3. Systems activity in axisymmetric strain: $\rho = -1/2$.

	Active systems	Activity conditions	Slip rates
0	$2^-3^+4^+5^-$	$-\sigma^2 = \sigma^3 = \sigma^4 = -\sigma^5 = \tau_0$	$\dot{\alpha}^2 \leq 0, \quad \dot{\alpha}^3 \geq 0, \quad \dot{\alpha}^4 \geq 0, \quad \dot{\alpha}^5 \leq 0$
θ_1	$2^-3^+4^+$	$-\sigma^2 = \sigma^3 = \sigma^4 = \tau_0$	$\dot{\alpha}^2 \leq 0, \quad \dot{\alpha}^3 \geq 0, \quad \dot{\alpha}^4 \geq 0,$
θ_2	$1^+3^+4^+$	$\sigma^1 = \sigma^3 = \sigma^4 = \tau_0$	$\dot{\alpha}^1 \geq 0, \quad \dot{\alpha}^3 \geq 0, \quad \dot{\alpha}^4 \geq 0$
θ_3	$1^+3^+5^+$	$\sigma^1 = \sigma^3 = \sigma^5 = \tau_0$	$\dot{\alpha}^1 \geq 0, \quad \dot{\alpha}^3 \geq 0, \quad \dot{\alpha}^5 \geq 0$
θ_4	$3^+4^-5^+$	$\sigma^3 = -\sigma^4 = \sigma^5 = \tau_0$	$\dot{\alpha}^3 \geq 0, \quad \dot{\alpha}^4 \leq 0, \quad \dot{\alpha}^5 \geq 0$
θ_5	$2^-3^+4^-5^+$	$-\sigma^2 = \sigma^3 = -\sigma^4 = \sigma^5 = \tau_0$	$\dot{\alpha}^2 \leq 0, \quad \dot{\alpha}^3 \geq 0, \quad \dot{\alpha}^4 \leq 0, \quad \dot{\alpha}^5 \geq 0$
$\pi - \theta_5$	$2^-4^-5^+$	$-\sigma^2 = \sigma^3 = \sigma^4 = \tau_0$	$\dot{\alpha}^2 \leq 0, \quad \dot{\alpha}^3 \geq 0, \quad \dot{\alpha}^4 \geq 0,$
$\pi - \theta_4$	$1^-2^-4^-$	$\sigma^1 = \sigma^3 = \sigma^4 = \tau_0$	$\dot{\alpha}^1 \geq 0, \quad \dot{\alpha}^3 \geq 0, \quad \dot{\alpha}^4 \geq 0$
$\pi - \theta_3$	$1^+2^-5^-$	$\sigma^1 = \sigma^3 = \sigma^5 = \tau_0$	$\dot{\alpha}^1 \geq 0, \quad \dot{\alpha}^3 \geq 0, \quad \dot{\alpha}^5 \geq 0$
$\pi - \theta_2$	$2^-3^+5^-$	$\sigma^3 = -\sigma^4 = \sigma^5 = \tau_0$	$\dot{\alpha}^3 \geq 0, \quad \dot{\alpha}^4 \leq 0, \quad \dot{\alpha}^5 \geq 0$
$\pi - \theta_1$	$2^-3^+4^+5^-$	$-\sigma^2 = \sigma^3 = \sigma^4 = -\sigma^5 = \tau_0$	$\dot{\alpha}^2 \leq 0, \quad \dot{\alpha}^3 \geq 0, \quad \dot{\alpha}^4 \geq 0, \quad \dot{\alpha}^5 \leq 0$
π			

Using the Tables 3 and 2 and the Eq. (2.6), we obtain easily the value of $\frac{\dot{\theta}}{E} = \frac{d\theta}{d\varepsilon}$ in each zone. The results are plotted in Fig. 7. This shows that the rotation stabilizes at three orientation limits: $\theta = \theta_s$, $\theta = 0$, $\theta = \pi - \theta_s$, with $\tan(2\theta_s) = 2\sqrt{2}$.

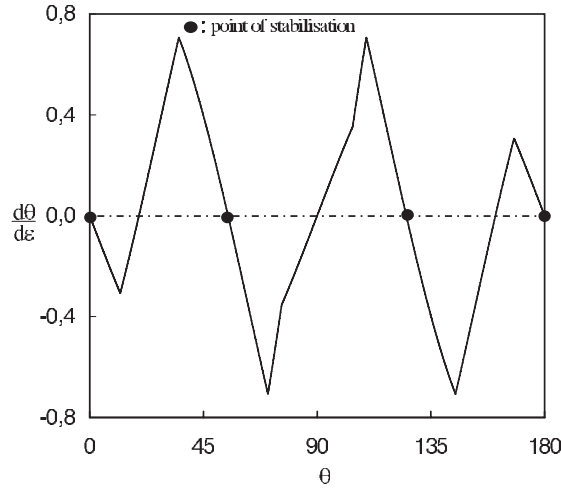


FIG. 7.

In the second illustrative example, a plane strain with $\rho = 0$ is considered, for which the strain rate components (Y_1, Y_2, Y_3) are defined by

$$Y_1 = \frac{1}{2}(1 + \cos(2\theta))E, \quad Y_2 = \frac{1}{2}(1 - \cos(2\theta))E, \quad Y_3 = +\frac{\sqrt{2}}{2}(\sin(2\theta))E.$$

Similarly to axisymmetric test, when θ goes from 0 to π , the resulting system's activity is summarized in Table 4 with $\tan(2\theta_6) = 2\sqrt{2}$.

Table 4. Systems activity in axisymmetric strain: $\rho = 0$.

	Active systems	Activity conditions	Slip rates
0	$2^-3^+5^+$	$-\sigma^2 = \sigma^3 = \sigma^5 = \tau_0$	$\dot{\alpha}^2 \leq 0, \quad \dot{\alpha}^3 \geq 0, \quad \dot{\alpha}^5 \geq 0$
$\pi - \theta_6$	$2^-3^+4^-5^+$	$-\sigma^2 = \sigma^3 = -\sigma^4 = \sigma^5 = \tau_0$	$\dot{\alpha}^2 \leq 0, \quad \dot{\alpha}^3 \geq 0, \quad \dot{\alpha}^4 \leq 0, \dot{\alpha}^5 \geq 0$
$\pi + \theta_6$	$2^-3^+4^-$	$-\sigma^2 = \sigma^3 = -\sigma^4 = \tau_0$	$\dot{\alpha}^2 \leq 0, \quad \dot{\alpha}^3 \geq 0, \quad \dot{\alpha}^4 \leq 0$
π			

The corresponding rate $\frac{\dot{\theta}}{E} = \frac{d\theta}{d\varepsilon}$ is plotted in Fig. 8. In this case the rotation stabilizes at two orientation limits $\theta = \theta_s$ and $\theta = \pi - \theta_s$, with $\tan(2\theta_s) = 2\sqrt{2}$.

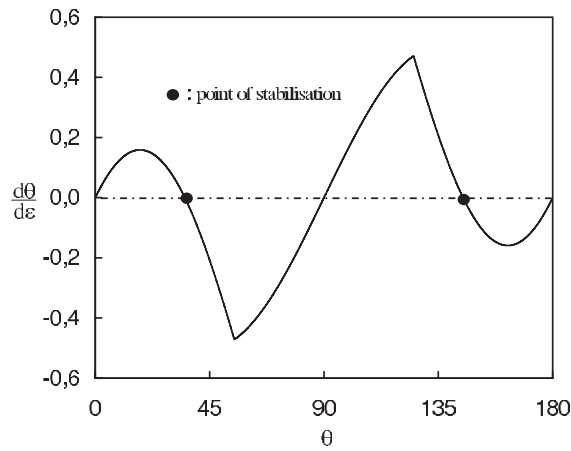


FIG. 8.

Finally, to complete the illustrative example, we analyse the case of strain test with $\rho = 1/2$. In this case, when θ goes from 0 to π , solely the regime $2^-3^+4^-5^+$ is potentially active and corresponds to one orientation limit $\theta = 0$. The curve $\dot{\theta}/E = d\theta/d\varepsilon$ is plotted in Fig. 9.

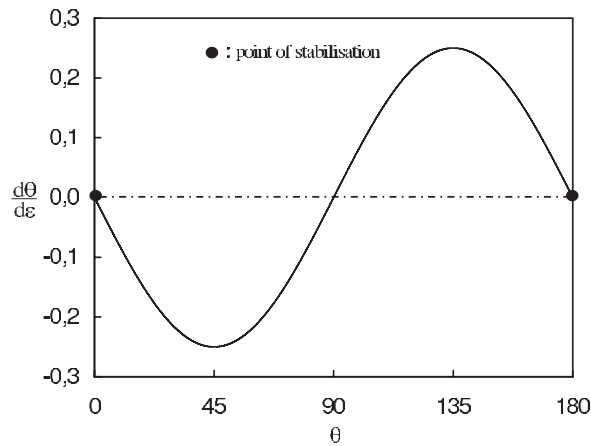


FIG. 9.

In Figs. 10, 11 and 12 we illustrate, for a given straining path ρ and initial orientation θ_0 , the lattice rotation in terms of the strain ε . The obtained results, which in fact do not depend on the hardening, show clearly that these two parameters θ_0 and ρ have an important influence on the stabilized rotation.

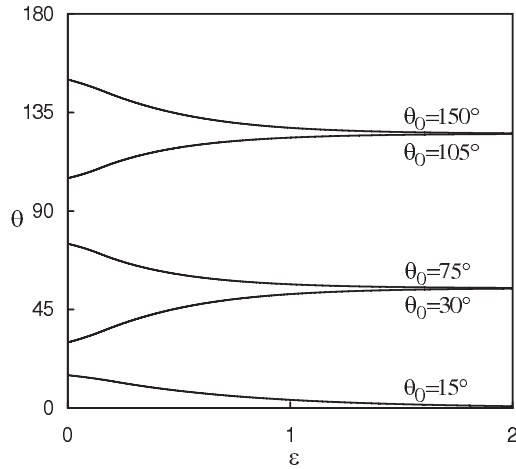


FIG. 10.

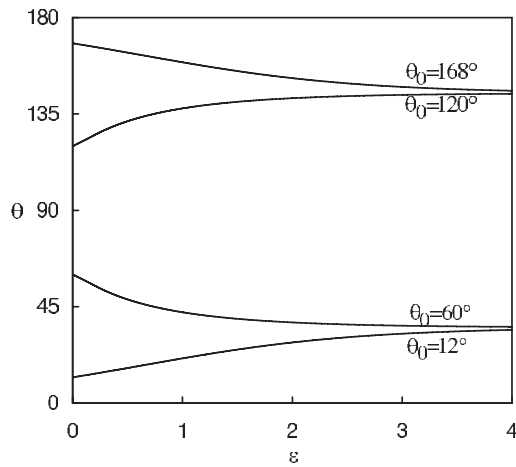


FIG. 11.

Generally, different situations may be encountered, according to the θ_0 and ρ values. For $-1 \leq \rho < 0$ and $0 < \rho \leq \frac{1 - \sqrt{3/2}}{1 + \sqrt{3/2}}$, the lattice orientation stabilizes

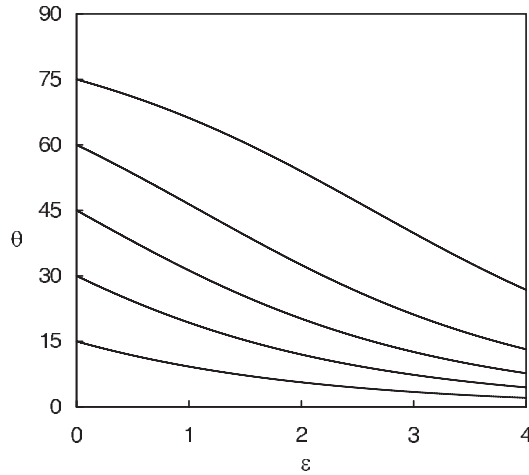


FIG. 12.

at three asymptotic values $\theta = 0$, $\theta = \theta_s$ and $\theta = \pi - \theta_s$, with

$$\tan(2\theta_s) = \frac{\sqrt{2}A + \sqrt{2}\sqrt{3 - 2A^2}}{2A - \sqrt{3 - 2A^2}}.$$

For $\rho = 0$, the stabilization at $\theta = 0$ disappears at remaining two angle limits $\theta = \theta_s$ and $\theta = \pi - \theta_s$, with $\tan(2\theta_s) = 2\sqrt{2}$. For $\rho \geq \frac{1 - \sqrt{3/2}}{1 + \sqrt{3/2}}$, only one orientation limit becomes possible $\theta = 0$.

5. Conclusion

In this paper the rigid-plastic single crystal, with or without isotropic hardening, is investigated. Our analysis is focused on the critical question corresponding to the slip systems activity and the indetermination problem due to the multiplicity of solutions.

Based on the plane single crystal model and the linear Bingham slip law, this problem is surmounted, by adopting the geometrical analysis in the strain rate space. The adjusted diagram activity is introduced, which determines a unique set of active slip systems. This proves that the linear viscoplastic analysis can be used as a new way for solving the indeterminacy problem.

As illustration, the biaxial extension is studied and the complete analytical solution of single crystal behavior is obtained. In particular, the analytical description of the plastic spin is introduced. The lattice orientation and the straining path have an important influence on the plastic spin evolution. Differ-

ent situations may be encountered, according to the strain path and the initial lattice orientation value. But in any case, this lattice rotation always stabilizes at a limit value resulting in a stabilized behavior for the crystal.

From this analysis, it is advisable to note the complexity of the plastic spin equation formulated phenomenologically, for representing different aspects of a single crystal. It must take into account, for a given structure, the orientation and the sollicitation path.

All of these calculations, which are performed in the framework of simple plane model, remain valid in the three-dimensional case. The plane single crystal model represents a reasonable compromise between the mathematical simplicity and the physical relevance for the analysis of some basic problems in the mechanics of single crystal.

Acknowledgements

This research is supported partially by the Morocco National Center for Scientific and Technique Research: PROTARS III Program N° D48/20 and SPI 04/06. The anonymous reviewers are gratefully acknowledged for their suggestions and valuable comments.

References

1. G.I. TAYLOR and C.F. ELAM, *The distortion of an aluminum crystal during a tensile test*, Proc. Royal Soc. London A **102**, 643–667, 1923.
2. G.I. TAYLOR and C.F. ELAM, *The plastic extension and fracture of aluminum single crystals*, Proc. Royal Soc. London A **108**, 28–51, 1925.
3. G.I. TAYLOR, *Plastic strain in metals* J. Institute of Metals, **62**, 307–324, 1938.
4. G.I. TAYLOR, *Analysis of plastic strain in cubic crystal*, Stephen Timoshenko 60th Anniversary, McMillan Co., New York, 218–224, 1938.
5. J. MANDEL, *Généralisation de la théorie de plasticité de W. T. Koiter*, Int. J. Solids Struct., **1**, 273–295, 1965.
6. R. HILL, *Generalized constitutive relations for incremental deformation of metal crystals by multislip*, J. Mech. Phys. Solids, **14**, 95–102, 1966.
7. J.R. RICE, *Inelastic constitutive relations for solids: an internal variable theory and its application to metal plasticity* J. Mech. Phys. Solids, **19**, 433–455, 1971.
8. R. HILL and J.R. RICE, *Constitutive analysis of elastic-plastic crystals at arbitrary strain*, J. Mech. Phys. Solids, **20**, 401–413, 1972.
9. F. SIDOROFF and C. TEODOSIU, *A theory of finite elasto-plasticity of single crystals*, Int. J. Engng. & Sci., **14**, 165–176, 1976.
10. R.J. ASARO and R.J. RICE, *Strain localisation in ductile single crystals*, J. Mech. Phys. Solids, **25**, 309–338, 1977.
11. R.J. ASARO, *Geometrical effects in the inhomogeneous deformation of ductile single crystals*, Acta Metall., **27**, 445–453, 1979.

12. R.J. ASARO, *Micromechanics of crystals and polycrystals*, Adv. Appl. Mech., **23**, 1–115, 1983.
13. K.S. HAVNER, *Finite Plastic Deformation of Crystalline Solids*, Cambridge University Press, 1992.
14. E. BUSO and G. CAILLETAUD, *On the selection of active slip systems in crystal plasticity*, Int. J. Plast., **7**, 11, 2212–2231, 2005.
15. P. FRANCIOSI and A. ZAOUI, *Crystal Hardening and the Issue of Uniqueness*, Int. J. of Plast., **7**, 4, 295–311, 1991.
16. D. PEIRCE, R. ASARO and A. NEEDLEMAN, *An analysis of nonuniform and localized deformation in ductile single crystals*, Acta Metall., **30**, 1087–1119, 1982.
17. Y.F. DAFALIAS, *Planar double-slip micromechanical model for polycrystal plasticity*, J. Engineering Mechanics, **119**, 1260–1284, 1993.
18. A. CLEMENT, *Prediction of deformation texture using a physical principle of conservation*, Mat. Sc. And Engrg., **55**, 203–233, 1982.
19. J. BOUKADIA and F. SIDOROFF, *Simple shear and torsion of a perfectly plastic single crystal in finite transformation*, Arch. Mech., **40**, 497–513, 1988.
20. J. BOUKADIA, A. CHENAOUI and F. SIDOROFF, *Simple shear in fcc single crystals at large deformations*, [in:] Proc. Int. Sem. MECAMAT'91 Fontainebleau (France) on Large Plastic Deformation, C. TEODOSIU, J.L. RAPHAEL & F. SIDIROFF [Eds.], Rotterdam Balkema, 109–116, 1993.
21. A. CHENAOUI, F. SIDOROFF and A. HIHI, *The texture evolution of planar polycrystal*, J. Mech. Phys. Solids, **48**, 2559–2584, 2000.
22. A. CHENAOUI, F. SIDOROFF, M. DARRIEULAT and A. HIHI, *The plane single crystal under off-axis tensile*, Archives of Mechanics, **54**, 3, 227–248, 2002, Warszawa.
23. R.J. ASARO and A. NEEDLEMAN, *Texture development and strain hardening in rate-dependent polycrystals*, Acta Metall., **33**, 923–953, 1985.
24. L. ANAND and M. KHOTARI, *A computational procedure for rate-independent crystal plasticity*, J. Mech. Phys. Solids, **44**, 4, 525–558, 1996.
25. E.C. BINGHAM, *Fluidity and Plasticity*, McGraw-Hill, New York, 215–218, 1922.
26. A.H. SHALABY and K.S. HAVNER, *A general kinematical analysis of double slip*, J. Mech. Phys. Solids, **26**, 79–92, 1978.
27. K.S. HAVNER, *The kinematics of double slip with application to cubic crystals in the compression test*, J. Mech. Phys. Solids, **27**, 415–429, 1979.
28. K.S. HAVNER, S.-C. WU and S. FUH, *On symmetric bicrystals at the yield point in (110) channel die compression*, J. Mech. Phys. Solids, **42**, 361–379, 1994.
29. K.S. HAVNER, *On velocity discontinuities in elastoplastic bicrystals in channel die compression*, Int. J. of Plasticity, **14**, 61–74, 1998.

Received January 22, 2008; revised version September 6, 2008.
